RSC Advances

PAPER

View Article Online
View Journal | View Issue

Cite this: *RSC Adv.*, 2023, **13**, 5667

Preparation of novel β-CD/P(AA-*co*-AM) hydrogels by frontal polymerization

Bin Li, Haibo Qin, Ming Ma, Xiaojia Xu, Mengjing Zhou, Wenrui Hao and Zhigang Hu

Received 1st December 2022
Accepted 8th February 2023

DOI: 10.1039/d2ra07649g

rsc.li/rsc-advances

In this paper, betaine (**Bet**) was used as a hydrogen bond acceptor (HBA), and acrylic acid (**AA**) and acrylamide (**AM**) were used as hydrogen bond donors (HBD) and mixed to form a deep eutectic solvent (DES). Different concentrations of β-cyclodextrin (β-CD) were dispersed in the DES, and a novel β-CD/P(**AA**-*co*-**AM**) hydrogel was prepared by frontal polymerization (FP). The characteristic structure and morphology of the hydrogels were analyzed using Fourier transform infrared (FTIR) spectroscopy and scanning electron microscopy (SEM), and the properties of the hydrogels were investigated. The results show that the mechanical properties of the hydrogel were improved by β-CD acting as a second cross-linking agent in the polymerization process, thus increasing the cross-link density of the hydrogel. Because the carboxyl groups contained in the acrylic acid dissociate under alkaline conditions, the composite hydrogel shows excellent pH responsiveness under alkaline conditions. Tetracycline hydrochloride was used as a drug model to test the drug loading and drug release performance of the hydrogels. With the increase of β-CD content, the loading capacity of the hydrogels for tetracycline hydrochloride gradually increased. The data of drug release indicated that the hydrogel has good drug delivery performance and has promising applications in drug delivery systems and other areas.

1. Introduction

A hydrogel is a cross-linked polymer with a three-dimensional network structure that can absorb a large number of water molecules without being soluble in water, and can have both solid and liquid properties. It has mechanical strength and wide ranging of stimulus responsiveness[1–3] and has physicochemical properties suitable for use in the human body.[4] Its unique network structure and properties can be used in many applications, such as in biomedicine,[5] drug delivery,[6–8] tissue engineering[9,10] and other fields. Typically, hydrogel networks are constructed from hydrophilic polymers, giving them a good ability to bind hydrophilic drugs.[11–13] However, the inability of the polymer network of hydrogels to bind drugs into the hydrogel leads to the inability of the hydrogel to control the drug release, limiting the application of hydrogels for drug delivery.

β-Cyclodextrin (β-CD) is a cyclic oligosaccharide with a hydrophobic cavity inside, allowing organic or inorganic molecules can be trapped.[14] The non-polar hydrophobic cavity of β-CD can absorb drug molecules into the hydrophobic cavity, forming an inclusion complex known as host–guest.[15] β-CD can be grafted through polymerization of β-CD to macromolecular chains, thus allowing the unique ability to form inclusion complexes to be transferred to the hydrogel. Moreover, the hydrophilic network of the hydrogel enhances the biocompatibility of β-CD and improves the stability of the inclusion complex, while β-CD enhances the mechanical of the hydrogel, and changes the release of the drug, which corresponds to an increase in the water solubility of the drug molecules and an increase in the drug loading capacity. Thus, β-CD is suitable for overcoming the limited absorption of hydrophobic drugs and the control of hydrophilic drug release.[16,17] The introduction of β-CD into polymeric matrices as polymeric fillers offers the possibility of preparing hydrogels with more excellent properties.

Hydrogels have various polymerization methods, such as suspension polymerization[18] and emulsion polymerization,[19] However, these polymerization methods have disadvantages such as difficult process control and impact on polymer performance. Frontal polymerization (FP) is primarily the conversion of monomers into polymers by the formation and propagation of thermal polymerization fronts using *in situ* self-propagation techniques and the ability to self-sustain and propagate in the region of the monomer mixture.[20] Compared with other polymerization methods, FP has process advantages such as shorter time, lower energy consumption, and no waste emission.[21] In recent years, frontal polymerization has synthesized numerous polymer hydrogels, such as poly (itaconic acid–acrylic acid–acrylamide) hydrogels[22] and poly (acrylic acid–acrylamide)/activated carbon.[23]

School of Mechanical Engineering, Wuhan Polytechnic University, Wuhan, Hubei, 430023, China. E-mail: libin_027@126.com

Deep eutectic solvent (DES) is a novel ionic liquid formed by mixing hydrogen bond acceptor (HBA) and hydrogen bond donor (HBD).[24] Its preparation method is relatively simple, only quaternary ammonium salts and HBD compounds are stirred at a certain temperature to form a eutectic mixture to obtain high purity DES. DES has low volatility, thermal stability, high electrical conductivity and good biocompatibility, which greatly facilitates the preparation of polymer hydrogels with excellent properties.[25–27]

Based on previous research, we prepared a novel β-CD/P(**AA**-*co*-**AM**) hydrogel with good drug release properties by using frontal polymerization in DES, and investigated the effect of β-CD content on the properties associated with the novel hydrogel. Frontal polymerization is a kind of polymerization method that uses the heat generated by the reaction of monomer polymerization as the driving force to gradually transform monomer into polymer. It only needs to trigger the monomer polymerization to release heat and generate the reaction front, and complete reactants can be formed within a few minutes. Therefore, frontal polymerization has a broad prospect for polymer application. We first prepared a ternary DES composed of acrylic acid–betaine–acrylamide, and then prepared β-CD/P(**AA-AM**) novel hydrogels by dispersing β-CD in the DES, Fourier Transform infrared spectroscopy (FTIR) and scanning electron microscopy (SEM) were used to characterize its structure, and further analyzed the effect law of β-CD on the mechanical properties and drug release properties of the hydrogels.

2. Materials and methods

2.1 Materials

Acrylamide (**AM**), betaine (**Bet**), β-cyclodextrin (β-CD) and acrylic acid (**AA**) were bought from Shanghai Aladdin Biochemical Technology Co. *N*,*N*-methylene bisacrylamide (MBA) was obtained from Tianjin Cameo Chemical Reagent Co., The potassium persulfate (KPS) was obtained from Sinopharm Chemical Reagent Co., All the reagents were of analytical grade and did not need further purification; the water used in this experiment was ultrapure water.

2.2 Synthesis of DES

Bet was used as HBA and **AM** and **AA** as HBD. The three raw materials were mixed in a molar ratio of 1 : 2 : 2 in a collector-type thermostatic heating magnetic stirrer with constant stirring until a uniform and transparent DES was formed (Fig. 1). The synthesized DES was allowed to stand until there were no air bubbles, and then β-CD was added to the DES according to the ratio in Table 1 with thorough stirring.

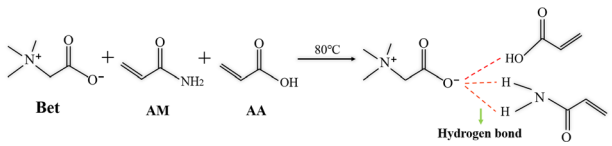

Fig. 1 Molecular formula for the formation of DES.

Table 1 Composition and proportion of hydrogels

Samples	AA/AM/Bet (Molar ratio)	β-CD (wt%)	MBA (wt%)	KPS (wt%)
FP0	2 : 2 : 1	0	1	0.5
FP1	2 : 2 : 1	0.25	1	0.5
FP2	2 : 2 : 1	0.50	1	0.5
FP3	2 : 2 : 1	1.00	1	0.5

2.3 Hydrogel preparation by frontal polymerization

The crosslinker and initiator were included in the mixture of DES and β-CD, mixed well and moved to a test tube (10 mm in diameter and 100 mm in length) and left for some time to remove the air bubbles generated during the stirring process. The heated electric soldering iron was leaned against the upper face of the solution for thermal triggering, and the upper end of the reactor was kept under atmospheric pressure, and the soldering iron was removed when the frontal appeared and the polymerization reaction started. After the reaction is completed, the prepared hydrogel is removed, cut into uniform discs and soaked in deionized water for one week to dissolve the unreacted monomers. The obtained novel hydrogels were dried in a freeze-dryer until the quality was constant and stored for the next test (Fig. 2).

2.4 Performance testing and characterization

2.4.1 Schematic diagram of the synthesis of novel hydrogels. In the FP reaction, the front end of the reaction moves toward the unreacted region at a constant rate, and the rate of frontal movement can be derived by recording the change in front end position at different times. To monitor the front-end temperature in relation to time, a test tube was held in a gripper at room temperature and a K-type thermocouple with a digital thermometer was dipped into the liquid to record the temperature of the front-end during the reaction.

2.4.2 SEM characterization. The cross-sections of the dried hydrogels were sprayed with gold using a high vacuum ion sputterer, and the microstructure of the hydrogels after gold spraying was observed by scanning electron microscopy (SEM).

2.4.3 FTIR characterization. Grinding of small pieces of dry hydrogel into powder, the spectral characteristics were evaluated using Fourier infrared spectroscopy between wave number 500 and 4000 cm^{-1}.

2.4.4 Mechanical performance testing. A universal testing machine was used to test the stress–strain properties of the composite hydrogel, and the prepared hydrogel samples were stretched at a speed of 100 mm min^{-1} until the hydrogel fractured, and the test was repeated several times. The hydrogel was tested for compression resistance using TA.XTC-18 texture analyzer. Before the test, the hydrogel was cut into a cylindrical shape of 10 mm in diameter and 10 mm in length, then immersed in deionized water for a period of time and compressed at a compression rate of 0.2 mm s^{-1} until the

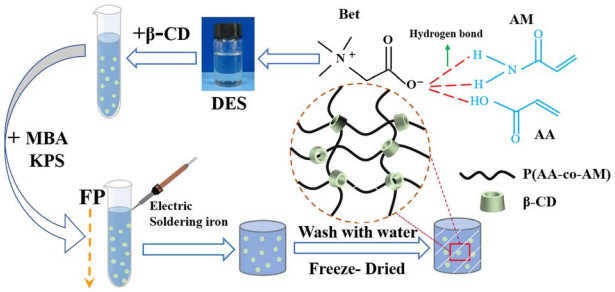

Fig. 2 Schematic diagram of the synthesis of novel hydrogels.

deformation of the hydrogel reached 80%, and the test was repeated several times. The formula for calculating the compressive strength of hydrogel to eqn (1):

$$P = \frac{F}{S} \tag{1}$$

In eqn (1), F is the applied force and S is the cross-sectional area of the hydrogel.

2.4.5 PH responsiveness performance test of hydrogel. Buffer solutions with pH 2.4, 4.5 (sodium citrate/citric acid) and pH 9.4, 10.7 (sodium carbonate/sodium bicarbonate) were prepared, and the pH of the buffer solutions was accurately tested with a digital pen acidity meter (PH-208, accuracy 0.01). The dry hydrogel with a mass of about 30 mg was put into the buffer solution until the swelling equilibrium was reached, and the water on the surface of the hydrogel was drained and weighed, and the equation for the swelling equilibrium (SR) was calculated to eqn (2):

$$\mathrm{SR} = \frac{m_t - m_0}{m_0} \tag{2}$$

In eqn (2), m_t is the swell weight of the hydrogel at different pH, m_0 is the dry weight of the hydrogel.

2.4.6 Drug loading. The dry gel was immersed in 40 ml (10 mg ml^{-1}) of tetracycline hydrochloride solution at 37 °C until the weight of the hydrogel did not change, the hydrogel was removed from the solution and the solution on the surface of the hydrogel was absorbed using filter paper, and the absorbance of the drug solution before and after the immersion of the hydrogel was measured to calculate the amount of drug absorbed.

2.4.7 Drug release performance testing. The fully drug loaded hydrogels were placed into 60 ml of deionized water at 37 °C. After a certain interval, 5 ml of drug release solution was taken out. The absorbance of the solution was measured at 357 nm with a UV-5900PC UV-visible spectrophotometer, and the solution was poured back into the container immediately after measurement. Linear regression was used to establish a pharmacokinetic model to study the drug release performance of hydrogels, and to calculate the cumulative release of drugs loaded on hydrogels. The drug release is calculated by the following equation is eqn (3).

$$\text{Cumulative Release}(\%) = \frac{W_{\text{drug}}}{W_{\text{gel}}} 100\% \tag{3}$$

In eqn (3), W_{drug} is the drug release at different times; W_{gel} is the total drug loading of the hydrogel.

3. Results and discussion

3.1 Measurement of frontal fronts

The frontal polymerization reaction creates a frontal front, which is an interface between the polymer produced by the reaction and the unreacted monomer. As illustrated in Fig. 3(a), the frontal position *versus* time curve shows that the frontal front moves toward the monomer region at a constant rate and completes the polymerization reaction rapidly in less than 6 min. As can be observed in Fig. 3(b), the frontal temperature change curve has a nearly horizontal section at the beginning, indicating that spontaneous polymerization has not occurred in FP.[28] As the β-CD content in the hydrogel increases, the movement of the frontal front decreases gradually, and V_f decreases from 2.82 to 1.41 cm min^{-1} when the β-CD content increases from 0 to 1wt%. The FP maximum temperature decreased from 168.7 °C to 142.3 °C. The increase of β-CD content decreased the V_f value because β-CD as an inert substance in the polymerization reaction would lead to thermal dispersion, which decreased the polymerization reaction temperature, thus slowing down the reaction rate, and the T_{max} value also decreased (Table 2).[29]

3.2 Fourier infrared spectroscopy (FTIR)

To further analyze the hydrogel condition, the hydrogel was analyzed by infrared spectroscopy, and the results are shown in Fig. 4. Fig. 4(a) shows the FTIR spectral profile of **AM**, the absorption peak at 3338 cm^{-1} is the stretching vibration peak of –NH_2 on the amide group (–$CONH_2$), and the absorption peak at 1664 cm^{-1} is the stretching vibration peak of C=O and the C=C vibration peak.[30,31] From Fig. 4(b), it can be seen that there is a strong absorption peak of P(**AA-AM**) at 3438 cm^{-1}, which corresponds to the stretching vibration peak of –NH_2 stretching vibration peak, and the absorption peak at 1647 cm^{-1} corresponds to the stretching vibration peak of C=O and C=C vibration peak. And the absorption peak at 2927 cm^{-1} is an asymmetric vibration of the C–H band, which is caused by the

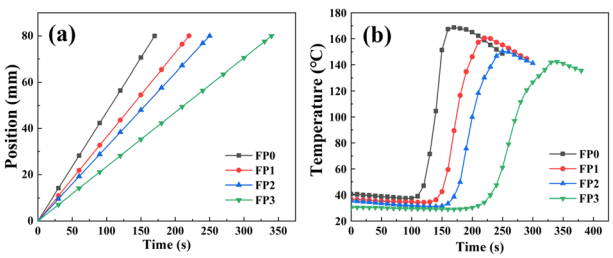

Fig. 3 (a) Speed of hydrogel polymerization frontal; (b) temperature of hydrogel polymerization frontal.

Table 2 Parameters of frontal polymerization

Sample	β-CD (wt%)	T_{max} (°C)	V_f (cm min^{-1})
FP0	0	168.7	2.82
FP1	0.25	160.6	2.18
FP2	0.50	150.3	1.92
FP3	1.00	142.3	1.41

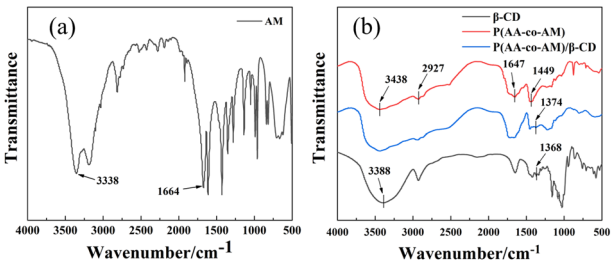

Fig. 4 (a) FTIR plots of acrylamide (**AM**); (b) FTIR plots of β-CD, P(**AA-AM**) and P(**AA-AM**)/β-CD.

cleavage of C=C in acrylamide.[32] The absorption peak present at 1449 cm^{-1} is a symmetric stretching peak formed by the dissociation of the hydroxyl group of **AM** into COO$^-$ during the polymerization process.[33] The IR spectral curve of β-CD shows that the absorption peak at 3388 cm^{-1} is the O–H stretching vibration peak, and the absorption peak at 1368 cm^{-1} is the bending vibration peak of O–H.[34] From the FTIR spectral profile of P(**AA-AM**)/β-CD, it can be seen that there are a large number of absorption peaks identical to those of P(**AA-AM**), but a stronger absorption peak appears at 1374 cm^{-1}, which corresponds to the bending vibration peak generated by O–H in β-CD. The above results indicate that β-CD enters in the polymer network of P(**AA-AM**) hydrogel.

3.3 Microscopic morphological of composite hydrogels (SEM)

To study the effect of β-CD on the internal structure of P(**AA-AM**) hydrogels, SEM observations were performed on the hydrolyzed composite hydrogels. Before performing SEM on the hydrogels, the hydrogels were pre-frozen after one week of immersion and subsequently freeze-dried at −60 °C for 48 h. After the freeze-drying treatment, the SEM scans of the four sets of hydrogels, the morphology is shown in Fig. 5. The cross section of FP0 appears to have folds, which may be caused by the collapse of the polymer network and the contraction of the structure during freezing. When the ice sublimates from the hydrogel, the flexible polymer chains in the hydrogel come into contact with each other, resulting in a collapsed hydrogel network.[35,36] The addition of β-CD makes the cross section of the hydrogel dense and smooth, which is due to the increased cross-link density of β-CD during polymerization, which contributes to the formation of a denser polymer network in the hydrogel, resulting in the contact between polymer chains becoming more frequent and the structure of the hydrogel becoming more dense.

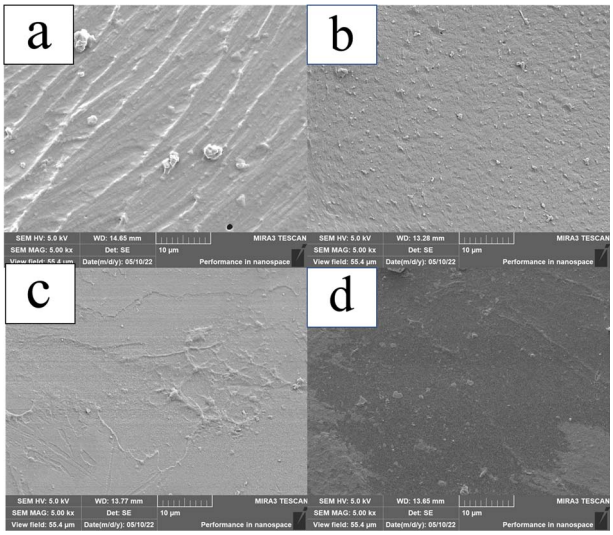

Fig. 5 SEM images of FP0 (a), FP1 (b), FP2 (c) and FP3 (d) for the freeze-dried hydrogels.

3.4 Mechanical properties

In order to test the mechanical properties of the hydrogels, tensile and compression experiments were performed on the hydrogels, and the experimental results are shown in Fig. 6. From Fig. 6(a), we can see that the tensile strength of the hydrogel gradually increases with the increase of β-CD in the hydrogel, and the highest tensile strength of FP3 hydrogel can reach 2.0 MPa, which is about two times of that of FP0 hydrogel. Fig. 6(b) shows the compression curve of the hydrogel, and the compressive strength of the hydrogel increases with the increase of β-CD. The above results show that the introduction of β-CD enhances the mechanical properties of the composite hydrogels, which is due to the role of β-CD as a chemical cross-linker in the polymerization process. The increase of β-CD content in the hydrogel network increases the cross-link density of the hydrogel. The higher the crosslinking density of the hydrogel, the denser the gel network formed, the more hydrogen bonds formed within and between molecules, and the stresses were dispersed at the fractures, resulting in the enhancement of the mechanical strength of the hydrogel.[37,38] The mechanical properties of hydrogels can usually be enhanced by increasing the concentration of hydroxyl groups of the constituent groups of polymeric materials, so the

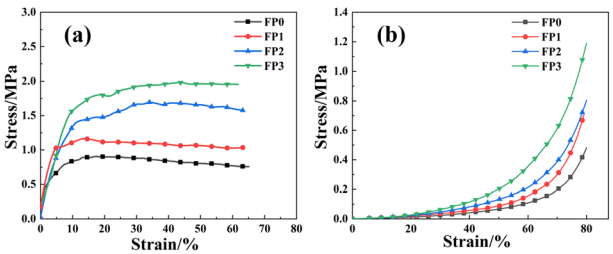

Fig. 6 (a) Hydrogel tensile property test curve; (b) hydrogel compression property test curve.

mechanical properties of hydrogels were also improved with the addition of β-CD.[39]

3.5 PH responsive

The effect of pH buffer solution on the dissolution equilibrium behavior of hydrogels is presented in Fig. 7. As can be observed in Fig. 7, the trend of hydrogel changes remained basically the same in solutions with different pH values. At pH 2.4, the carboxylic acid groups exist in the form of –COOH, which reduces the electrostatic repulsive force of the polymer chains and causes the polymer chains of the whole hydrogel network to be intertwined and contracted, so the swelling capacity of the hydrogel is low at low this environment.[40] When the pH is at 4.8 environment, the functional groups start to dissociate, the hydrogen bonding between –COOH groups is weakened, and the osmotic pressure inside the hydrogel gradually increases, leading to an increase in ESR.[33] The reduced swelling behavior at pH 7 is probably due to the presence of hydrogen bonding between $-CONH_2$ groups and –COOH groups, which leads to increased crosslinking density and shrinkage of the polymer network.[31] When the pH is greater than 7, the carboxylic acid groups ionize, –COOH dissociates into $-COO^-$, and the ions between generates strong electrostatic repulsion, which expands the polymer network and thus leads to an increase in osmotic pressure inside the hydrogel, resulting in an increase in the swelling rate of the hydrogel. As can be show in Fig. 7, the swelling rate of the hydrogel gradually decreases with the increase of β-CD content, which is because the increase of β-CD content increases the cross-link density of the hydrogel, while the hydrophobic cavity of β-CD can prevent water molecules from penetrating into the hydrogel, thus limiting the swelling performance of the hydrogel.[41]

3.6 Drug loading of hydrogels

We chose tetracycline hydrochloride as the model drug and loaded it into the hydrogel. Fig. 8 shows the drug loading data of

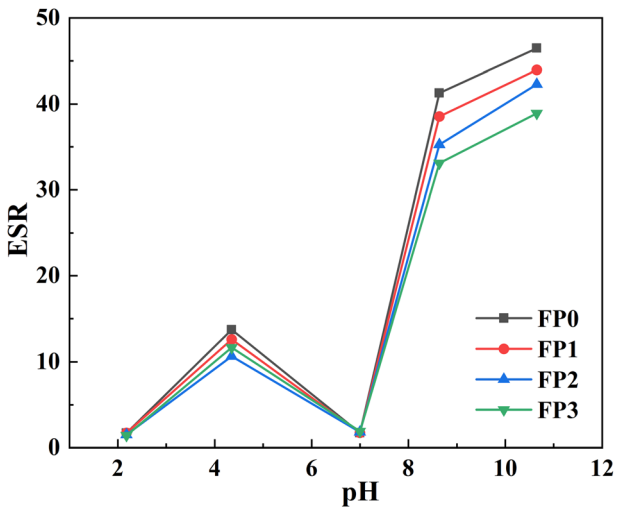

Fig. 7 pH responsiveness curve of hydrogels.

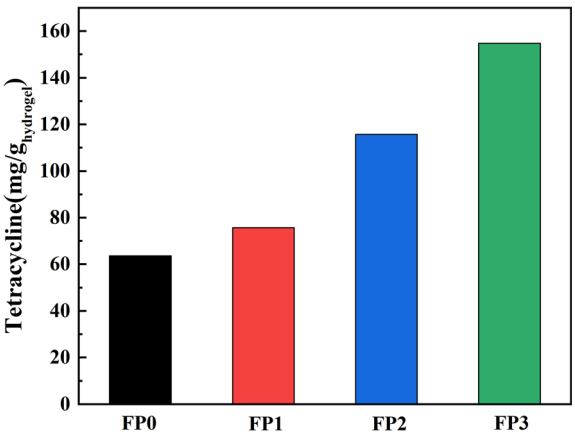

Fig. 8 Drug loading of hydrogels.

the hydrogel, the drug loadings of FP0, FP1, FP2 and FP3 were 63.51, 75.61, 115.63 and 154.67 mg g^{-1}, with the increase of β-CD content, the loading of the hydrogel to the drug increased. Fig. 9 shows a schematic diagram of the uptake of drug molecules by the hydrogel. β-CD/P(**AA**-*co*-**AM**) composite hydrogel is loaded with drug mainly by two ways. One is, the hydrogel swelling leads to the drug-containing solution into the hydrogel network; the other is, the hydrophobic cavity of β-CD can bind to the hydrophobic end of tetracycline hydrochloride, so that β-CD can form host–guest inclusion complexes with drug molecules, increasing the affinity of the polymer network for drug molecules and increasing the number of drug molecules captured by the hydrogel, thereby enhancing the drug adsorption capacity of the hydrogel.[42,43] The increase in β-CD content in the hydrogels allowed more drugs to be loaded into the polymer network, improving the drug loading of the hydrogels. Fig. 9 is a schematic diagram of drug encapsulation by hydrogel, β-CD can form a 1 : 1 inclusion complex with the guest molecule. If the guest molecule is too large to accommodate a cyclodextrin hole, the unincluded end will provide another site of action, so that the host guest molecule can form the complex at a 2 : 1 mass ratio.[44]

3.7 Drug release of hydrogels

The cumulative drug release rate of the hydrogel is shown in Fig. 10 by performing drug release tests on the hydrogel, thereby investigating the effect produced by β-CD on drug release. In drug release studies, when deionized water penetrates into the polymer matrix, the trapped drug molecules are released from

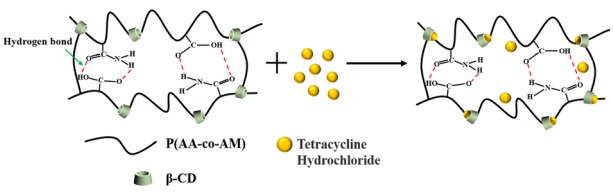

Fig. 9 Schematic diagram of the absorption of drug molecules by hydrogels.

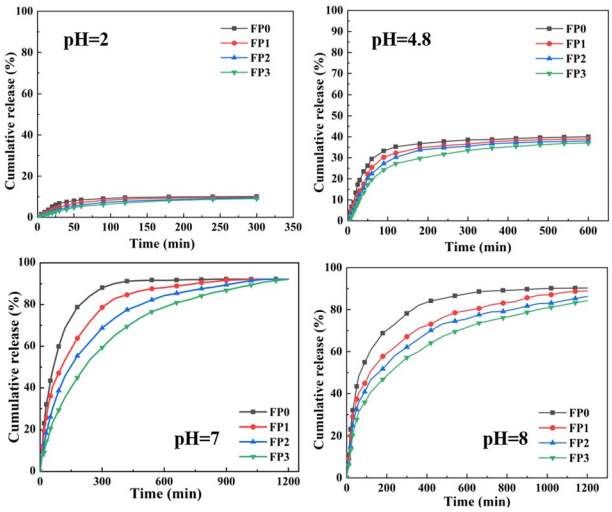

Fig. 10 Drug release profile of hydrogels.

the hydrogel due to diffusion that occurs due to osmotic pressure. As can be shown in Fig. 10, the drug release efficiency of the hydrogels showed a significant difference with the increase of β-CD content in the hydrogels, and the drug release rate gradually decreased. At the beginning, the greater osmotic pressure between the drug molecules in the hydrogel network and the external environment resulted in a greater drug release velocity from the hydrogel within 600 min, while after 600 min, the drug release velocity from the hydrogel started to decrease. β-CD content increases the cross-link density of the hydrogel and makes the polymeric network of the polymer more compact, resulting in a restricted rate of water entry into the hydrogel, thus making the drug molecule's slow release time becomes longer.[45–47] It can be seen from the graph that the drug release increases significantly as the pH becomes larger. β-CD contains a large number of –OH and CH_2OH groups in its structure, which makes the hydrogel hydrophilic. At low pH, these groups remain bound and therefore drug release is low. As the pH increases, the groups are ionized and the repulsive forces and osmotic pressure within the hydrogel network increase, resulting in an increase in the solubilization equilibrium of the hydrogel, which leads to an increase in drug release.[48]

4. Conclusions

In this paper, β-CD was mixed with **Bet-AA-AM** ternary DES to prepare new β-CD/P(**AA**-*co*-**AM**) hydrogels by front-end polymerization, and the structure and properties of the hydrogels were investigated, and the results showed that:

(1) Compared with the conventional polymerization method, FP prepared composite hydrogels with faster polymerization rate and greener raw materials. A new hydrogel of β-CD/P(**AA-AM**) was prepared by frontal polymerization, and after the addition of β-CD, the polymerization rate of the hydrogel gradually decreased due to the thermal diffusion of β-CD.

(2) The mechanical properties of the hydrogels were gradually improved with the addition of β-CD. The addition of β-CD increased the cross-link density of the hydrogels and increased the number of hydrogen bonds in the hydrogels, which led to the improvement of the mechanical properties of the hydrogels.

(3) β-CD controls the release behavior of drug molecules by forming host–guest inclusion complexes. When β-CD is added to the hydrogel it can make the hydrogel have drug retardation, and after loading the composite hydrogel with drug, it can achieve prolonged release in deionized water, making the hydrogel potentially useful for applications such as drug delivery systems.

Author contributions

B. L., proposed the ideas, steps and details of the experiment, most of the experiments were done by H. B. Q., M. J. Z, X. J. X., W. R. H., where H. B. Q was instrumental in the proper conduct of the experiments and wrote the article together with B. L., and all the authors analyzed the data, discussed the conclusions.

Conflicts of interest

The authors declare that they have no relevant financial or non-financial interests to disclose.

Acknowledgements

The work is supported by 2022 Knowledge Innovation Dawn Special Plan Project (2022010801020393), Marine Defense Technology Innovation Center Innovation Fund (JJ-2020-719-01), Natural Science Foundation of Hubei Province (2021CFB292) and Research and Innovation Initiatives of WHPU (2022J04). This work was finished at Wuhan Polytechnic University, Wuhan.

Notes and references

1 Y. Huang, H. Yu and C. Xiao, *Carbohydr. Polym.*, 2007, **69**(4), 774–783.
2 M. C. Koetting, J. T. Peters, S. D. Steichen and N. A. Peppas, *Mater. Sci. Eng., R*, 2015, **93**, 1–49.
3 X. Xiong, C. Wu, C. Zhou, G. Zhu, Z. Chen and W. Tan, *Macromol. Rapid Commun.*, 2013, **34**(16), 1271–1283.
4 J. Kopecek, *J. Polym. Sci., Part A: Polym. Chem.*, 2009, **47**(22), 5929–5946.
5 A. K. Gaharwar, N. A. Peppas and A. Khademhosseini, *Biotechnol. Bioeng.*, 2014, **111**(3), 441–453.
6 T. Don, M. Huang, A. Chiu, K. Kuo, W. Y. Chiu and L. H. Chiu, *Mater. Chem. Phys.*, 2008, **107**, 266–273.
7 R. Machín, J. R. Isasi and I. Vélaz, *Carbohydr. Polym.*, 2012, **87**(3), 2024–2030.
8 T. R. Thatiparti and H. A. von Recum, *Macromol. Biosci.*, 2010, **10**(1), 82–90.

9 X. Li, Y. Weng, X. Kong, B. Zhang, M. Li, K. Diao, Z. Zhang, X. Wang and H. Chen, *J. Mater. Sci.: Mater. Med.*, 2012, **23**(12), 2857–2865.
10 Z. Xu, G. Liu, Q. Li and J. Wu, *Nano Res.*, 2022, **15**(6), 5305–5315.
11 Y. Zhang, L. Tao, S. Li and Y. Wei, *Biomacromolecules*, 2011, **12**(8), 2894–2901.
12 J. Wu, X. Zhao, D. Wu and C. Chu, *J. Mater. Chem.*, 2014, **2**, 6660–6668.
13 K. S. Soppimath, T. M. Aminabhavi, A. M. Dave, S. G. Kumbar and W. E. Rudzinski, *Drug Dev. Ind. Pharm.*, 2002, **28**(8), 957–974.
14 A. Roy, K. Manna, S. Dey and S. Pal, *Carbohydr. Polym.*, 2023, **306**, 120576.
15 P. Gami, D. Kundu, S. D. K. Seera and T. Banerjee, *Int. J. Biol. Macromol.*, 2020, **158**, 18–31.
16 A. Concheiro and C. Alvarez-Lorenzo, *Adv. Drug Delivery Rev.*, 2013, **65**(9), 1188–1203.
17 H. Zhao, J. Gao, R. Liu and S. Zhao, *Carbohydr. Res.*, 2016, **428**, 79–86.
18 H. Liu, C. Wang, Q. Gao, X. Liu and Z. Tong, *Acta Biomater.*, 2010, **6**(1), 275–281.
19 A. C. Nalawade, R. V. Ghorpade, S. Shadbar, M. S. Qureshi, N. N. Chavan, A. A. Khan and S. Ponrathnam, *J. Mater. Chem. B*, 2016, **4**(3), 450–460.
20 J. A. Pojman, V. M. Ilyashenko and A. M. Khan, *J. Chem. Soc., Faraday Trans.*, 1996, **92**, 2825–2837.
21 Q. Li, H. X. Shen, C. Liu, C. F. Wang, L. Zhu and S. Chen, *Prog. Polym. Sci.*, 2022, **127**, 101514.
22 M. Irfan, X. Y. Du, X. R. Xu, R. Q. Shen, S. Chen and J. J. Xiao, *J. Polym. Sci., Part A: Polym. Chem.*, 2019, **57**(22), 2214–2221.
23 S. Li, H. Huang, M. Tao, X. Liu and T. Cheng, *J. Appl. Polym. Sci.*, 2013, **129**(6), 3737–3745.
24 Q. Zhang, K. De Oliveira Vigier, S. Royer and F. Jerome, *Chem. Soc. Rev.*, 2012, **41**(21), 7108–7146.
25 F. del Monte, D. Carriazo, M. C. Serrano, M. C. Gutierrez and M. L. Ferrer, *ChemSusChem*, 2014, **7**(4), 999–1009.
26 A. Paiva, R. Craveiro, I. Aroso, M. Martins, R. L. Reis and A. R. C. Duarte, *ACS Sustainable Chem. Eng.*, 2014, **2**(5), 1063–1071.
27 E. L. Smith, A. P. Abbott and K. S. Ryder, *Chem. Rev.*, 2014, **114**(21), 11060–11082.
28 S. Li, H. Zhang, J. Feng, R. Xu and X. Liu, *Desalination*, 2011, **280**, 95–102.
29 D. Nuvoli, V. Alzari, L. Nuvoli, M. Rassu, D. Sanna and A. Mariani, *Carbohydr. Polym.*, 2016, **150**, 166–171.
30 M. Yu and M. Liu, *Chem. Res. Chin. Univ.*, 2019, **35**(2), 311–318.
31 B. Li, X. Xu, Z. Hu, Y. Li, M. Zhou, J. Liu, Y. Jiang and P. Wang, *RSC Adv.*, 2022, **12**(30), 19022–19028.
32 J. Z. Yi and L. M. Zhang, *Eur. Polym. J.*, 2007, **43**(8), 3215–3221.
33 S. Nesrinne and A. Djamel, *Arabian J. Chem.*, 2017, **10**(4), 539–547.
34 M. A. Medeleanu, D. I. Hadaruga, C. V. Muntean, G. Popescu, M. Rada, A. Heghes, S. E. Zippenfening, C. A. Lucan Banciu, A. B. Velciov, G. N. Bandur, N. G. Hadaruga and M. Rivis, *Carbohydr. Polym*, 2021, **265**, 118079.
35 S. Huang, Z. Zhao, C. Feng, E. Mayes and J. Yang, *Composites, Part A*, 2018, **112**, 395–404.
36 Y. Zhang, L. Ye, M. Cui, B. Yang, J. Li, H. Sun and F. Yao, *RSC Adv.*, 2015, **5**(95), 78180–78191.
37 Q. Gao, J. Hu, J. Shi, W. Wu, D. K. Debeli, P. Pan and G. Shan, *Soft Matter*, 2020, **16**(46), 10558–10566.
38 F. van de Manakker, L. M. J. Kroon-Batenburg, T. Vermonden, C. F. van Nostrum and W. E. Hennink, *Soft Matter*, 2010, **6**(1), 187–194.
39 D. Jeong, S. W. Joo, Y. Hu, V. V. Shinde, E. Cho and S. Jung, *Eur. Polym. J.*, 2018, **105**, 17–25.
40 A. Roy, P. P. Maity, A. Bose, S. Dhara and S. Pal, *Mater. Chem. Front.*, 2019, **3**(3), 385–393.
41 X. Yang and J. C. Kim, *Biotechnol. Bioeng.*, 2010, **106**(2), 295–302.
42 Y. Wang, N. Yang, D. Wang, Y. He, L. Chen and Y. Zhao, *Polym. Degrad. Stab.*, 2018, **147**, 123–131.
43 J. Xu, X. Li, F. Sun and P. Cao, *J. Biomater. Sci., Polym. Ed.*, 2010, **21**, 1023–1038.
44 G. Wenz, B. Han and A. Muller, *Chem. Rev.*, 2006, **106**, 782–817.
45 A. Abou-Okeil, M. Rehan, S. M. El-Sawy, M. K. El-bisi, O. A. Ahmed-Farid and F. A. Abdel-Mohdy, *Eur. Polym. J.*, 2018, **108**, 304–310.
46 Kiran, R. Tiwari, V. K. Singh, M. K. Singh, S. Krishnamoorthi and K. Kumar, *Iran. Polym. J.*, 2020, **29**(7), 615–623.
47 N. S. Malik, M. Ahmad and M. U. Minhas, *PLoS One*, 2017, **12**(2), e0172727.
48 S. A. Khan, W. Azam, A. Ashames, K. M. Fahelebom, K. Ullah, A. Mannan and G. Murtaza, *J. Drug Delivery Sci. Technol.*, 2022, **60**, 101970.